Environmental Science
Water Research & Technology

ROYAL SOCIETY OF CHEMISTRY

PAPER

View Article Online
View Journal | View Issue

Cite this: *Environ. Sci.: Water Res. Technol.*, 2021, **7**, 562

Water quality changes during the first meter of managed aquifer recharge†

Kristofer Hägg, *[ab] Jing Li,[ab] Masoumeh Heibati,[c] Kathleen R. Murphy,[c] Catherine J. Paul[a] and Kenneth M. Persson[a]

Received 14th September 2020,
Accepted 11th February 2021

DOI: 10.1039/d0ew00839g

rsc.li/es-water

The capacity of an artificial recharge field to alter organic matter and the bacterial flora of surface water was assessed by following changes in bacterial communities and composition of natural organic matter (NOM) over the first meter of infiltration depth. The sampling strategy applied in this study ensured that water samples consisted only of infiltrated water, excluding natural groundwater. Water was sampled at 50 and 100 cm below the surface of an infiltration basin divided into two halves; one side was dried and frozen and one was infiltrating water during the winter period prior to the sampling period. Bacterial cell counts, proportions of intact cells and community fingerprints were determined by flow cytometry, and NOM was characterized using total organic carbon (TOC), $UV_{254\ nm}$-absorbance (UVA) and fluorescence spectroscopy. Around 40% of the NOM was removed after only 50 cm. Protein-like components were reduced to a larger extent (45–50%) than the humic-like components (25%), suggesting removal of mostly biodegradable fractions of NOM. After only 50 cm of infiltration, about 99% total cell count (TCC) was removed. The flow cytometric data revealed that the bacterial communities collected after infiltration from the basin area that had been dried and frozen were more similar to those in the raw water. This suggests that drying and freezing the basin negatively impacted its treatment capacity. The results from this study highlight the importance of a well-developed biofilm and unsaturated zone for artificial recharge.

Water impact

We believe that this paper increases our understanding of the chemical and microbial changes that occur during managed aquifer recharge, and the impact management of infiltration basins has on potable water quality. The results from this study could give operators tools to improve the capacity of water treatment plants and thereby aid in securing water supply for growing populations.

1 Introduction

Managed aquifer recharge (MAR) is a common way of producing drinking water in Sweden,[1] Europe and the world,[2,3] where water treatment plants (WTPs) recharge the groundwater by infiltrating surface water through infiltration basins. The technique utilizes the natural biological treatment processes that occur when surface water slowly infiltrates and percolates through surface soils and becomes groundwater. During infiltration, natural organic matter (NOM), bacteria and viruses are removed,[4] and a substantial part of the removal is thought to occur in the top unsaturated and biologically active layer.[5–7] The accumulation of NOM and biomass on the bottom of the basin slows the infiltration rate and therefore introduces oxygen under the infiltration basins, creating an unsaturated zone.[8] In general, over 50% of NOM is removed during artificial recharge,[4,9–11] although this percentage varies depending on soil composition, infiltration rates, temperatures, distance between recharge area and sampling points, mixing of artificial and natural groundwater, and biofilm development. The latter is particularly important for removal of small particles, such as bacteria and viruses, considering the comparably large pore size (around 60 μm for slow sand filters) of the sand beds.[5]

Groundwater recharge is similar to slow sand filtration (SSF), where well-developed biofilms are important for their performance, for the removal of organic matter and microorganisms.[12] Biofilms improve not only the function of

[a] *Division of Water Resources Engineering, Faculty of Engineering LTH, Lund University, John Ericssons Väg 1, V-Hus, 221 00 Lund, Sweden. E-mail: kristofer.hagg@tvrl.lth.se, lijingnice@gmail.com, catherine.paul@tvrl.lth.se, Kenneth_m.persson@tvrl.lth.se*
[b] *Sweden Water Research AB, Ideon Science Park, Scheelevägen 15, 223 70 Lund, Sweden*
[c] *Division of Water Environment Technology, Department of Architecture and Civil Engineering, Chalmers University of Technology, Sven Hultins gata 8, 412 96 Gothenburg, Sweden. E-mail: heibati@chalmers.se, murphyk@chalmers.se*
† Electronic supplementary information (ESI) available. See DOI: 10.1039/d0ew00839g

SSFs but also the functioning of granulated active carbon filters (GACs) and rapid sand filters (RSFs).[13] Flow cytometry has been used to look more closely at microbial communities in water supply systems: including the influence of biofilms in sand filters[12,13] and distribution systems[14] on microbial communities in drinking water was shown. Flow cytometry has also been used to monitor microbial communities in other contexts, such as microbial breakthroughs to the groundwater after precipitation.[15]

The strategy of artificially infiltrating water from various sources to replenish the natural groundwater and using aquifers for water supply storage, seasonally or year round, is suggested as one potential strategy for mitigating water shortage for irrigation and other uses.[16,17] However, little is known about the specifics of when surface water becomes groundwater during managed aquifer recharge (*e.g.* through infiltration basins). This is an important aspect, not only for seasonal water storage but also for MAR plants. Numerous studies have been published on the treatment performance of groundwater recharge by comparing surface water quality and water collected in wells.[4,9–11,18–20]

Several studies have investigated chemical and microbial changes during infiltration in soil columns and infiltration fields,[4,21] however, little is known about specific structural changes in organic matter and microbial communities in the natural environment without the interference of natural groundwater. Understanding these processes can inform management strategies and optimization of MAR. This study investigates compositional changes and removal of NOM and bacteria during the first 1 m of MAR. The hypothesis was that different management processes of the infiltration basin, such as drying and freezing, would impact treatment performance and that this impact would be clearly described by the sampling strategy applied in this study. As the location of the samplers ensured that water samples consisted only of infiltrated water, excluding natural groundwater, changes introduced only to the filtrate water quality during the first metre of infiltration to be determined.

2 Materials and methods

2.1 Site description

This study was conducted at Vomb Water Works, an MAR plant in southern Sweden with 54 infiltration basins excavated in an infiltration field of glaciofluvial deposits[22] (ESI† Fig. A1). Source water from Lake Vomb is pretreated by micro sieving (40 μm) before the water is channeled to the infiltration basins. Once in the basins, the lake water infiltrates at a rate of approximately 0.4 m d^{-1} and becomes groundwater. After about two to three months the water is collected in 114 wells located about 200 meters from the ponds and pumped to the treatment plant, where the groundwater is aerated, softened and filtered through rapid sand filters (RSFs) before adding monochloramine and pumping it out to the municipalities.[23] Maintenance of the recharge ponds follows certain seasonal patterns, whereby basins are taken into operation in late autumn–winter to ensure the development of the biofilm before algae blooms in late summer. Once there is too much resistance in the bottom of the basin (bioclogging), usually after about 1.5 year, they are emptied, skimmed and allowed to dry and freeze over winter. The reason for this is to increase permeability through drying and cracking the bottom of the basins.

The catchment area around Lake Vomb is dominated by agricultural land,[24] which causes the lake to be hypertrophic and strong seasonal algae blooms.[18,25] As a result, the lake experiences a high turnover of organic matter, and receives substantial amount of organic matter originating from the agricultural land. The small amount of forest in the catchment area results in comparatively lower amounts of humic acid in the lake.

In this study, an infiltration basin was divided into two halves, A and B (Fig. 1). Basin A was treated the same way as the other infiltration basins at the water treatment plant (WTP) at the time of the study. The top 5 cm of the basin surface was skimmed after allowing the basin to dry and freeze over winter. Basin B was skimmed without freezing. This was achieved by continuing to feed water into the basin throughout winter. Both halves received pretreated water filtered through 40 μm disc filters, and taken into operation (May 28th, 2018) at the same time.

2.2 Water sampling

Tension-free soil solution collectors (Prenart soil solution collectors, Prenart Equipment APS, Denmark; Buckingham *et al.*, 2008)[26] were installed below the surface under the infiltration basin but above the natural groundwater table at two different depths and on both A and B sides; 50 and 100 cm, for a total of 16 samplers (A1-50, A1-100, A2-50, A2-100, A3-50, A3-100, A4-50, A4-100, B1-50, B1-100, B2-50, B2-100, B3-50, B3-100, B4-50 and B4-100) (Fig. 1). All samplers were installed in a line, 5 m between each sampler pair (*i.e.* A1-50 and A1-100), stretching away from the water inlet. A1-50, for example, refers to the first sampler 5 m away from the inlet at 50 cm below the surface under basin A. A-50 and B-50

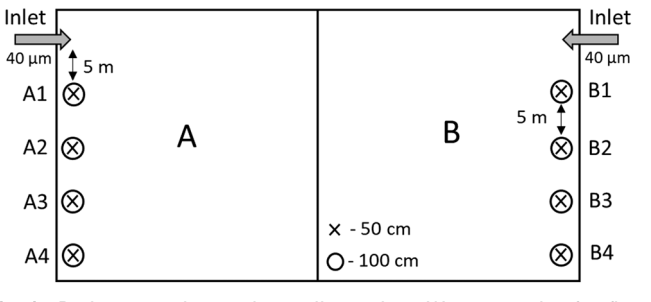

Fig. 1 Project overview and sampling points. Water samples for flow cytometry measurements were taken from the inlet, samplers A3, A4, B3 and B4 at 50 and 100 cm. Water samples for all chemical measurements were taken from the inlet, all soil water samplers, basin A and B.

refers to all the samplers at 50 cm under basin A and B. Each sampler was connected by a Teflon tube to a 2 liter collection bottle. Vacuum was applied to the bottles using a vacuum pump. Samples were collected from each sampler, source water (raw water entering basin B after the 40 μm microsieves) and both basins once a week from the July 4th to November 21st, 2018. The total amount of samples from each sampling point (19 locations) and for each measurement was 19 (one every week), where triplicates were taken for each sample. Water samples for fluorescence spectroscopy were collected for three weeks from 7th to 21st of November from the raw water, samplers B2-50, B2-100, B3-50, B3-100, B4-50 and B4-100.

The day before samples were collected, vacuum (−0.6 bar) was applied to each sample collection bottle to ensure adequate sample volume. The following day, water for NOM analysis was collected from all the bottles. Chromophoric dissolved organic matter (CDOM) Samples were collected in ashed amber glass bottles and stored at 4 °C until measurement. Vacuum was applied again on half the samplers (A3-50, A3-100, A4-50, A4-100, B3-50, B3-100, B4-50 and B4-100), and 3 mL samples were collected in sterile falcon tubes incased in 50 mL tubes with a membrane lid, for flow cytometry. All samples were ice cooled and stored overnight at 4 °C until analyses. All water samples taken from the groundwater, *i.e.* from the soil water samplers, are referred to as infiltrated water, and samples taken from the source water, *i.e.* filtered water from Lake Vomb, are referred to as raw water. The samples taken from the infiltration basins are referred to as basin water.

Two samplers seen in ESI† Fig. A2a (B2-50 and B2-100) and three samplers seen in ESI† Fig. A2b (B1-50, B2-50 and B2-100) initially showed higher values (TOC and UVA) than the raw water, indicating that there were sources of NOM additional to the raw water. This was likely caused by organic matter in the soil in those locations. The three samplers (B1-50, B2-50 and B2-100) were therefore excluded for the whole study period. Additionally, no infiltrated water samples were could be taken from sampler A1-100. ESI† Fig. A3 shows the results (including all samplers) from the TOC (ESI† Fig. A2a) and UVA (ESI† Fig. A2b) measurements.

2.3 Analytical methods

2.3.1 Flow cytometry analysis. Water samples were measured for total cell count (TCC) and intact cell count (ICC) using the dyes SYBR Green I and propidium iodide (PI) (Sigma-Aldrich, Germany), according to ref. 12, 27 and 28. For measurements of TCC, 495 μL water sample at room temperature was added to a 5 μL 1 : 100 mixture of SYBR Green I (10 000×) and dimethyl sulfoxide DMSO, resulting in a 1× SYBR Green I final concentration. For measurements of ICC, 494 μL water sample at room temperature was added to a 6 μL 1 : 6 (50 to 250 μL) mixture of PI and 100× SYBR Green I, to a final PI and SYBR Green I concentration of 3 μM and 1×, respectively. After the dye addition, the samples were vortexed and incubated in the dark for 15 min at 37 °C. After incubation, the samples were vortexed again and analysed using a BD Accuri C6 plus flow cytometer (BD Bioscience) equipped with a 50 mW laser (488 nm). For each sampling rack, Millipore water was placed between triplicates of water samples, and 50 μL was analysed for each water sample. The TCC, ICC, fluorescent fingerprint, low (LNA) and high nucleic acid (HNA) content were calculated and determined based on gating strategies according to Prest *et al.* (2013),[28] using one defined gate for all samples. Additional gates were applied to the water samples to follow specific changes in bacterial community populations in the raw water. The applied gates were low LNA (L-LNA), high LNA (H-LNA) and new HNA (N-HNA) and can be seen in ESI† Fig. A3. The data was processed using FlowJo software from Tree Star Inc, USA.

2.3.2 Chemical analysis. Optical properties (absorbance and fluorescence) of the dissolved organic matter (DOM) were measured within 48 hours after sampling. Prior to measurements, the water samples were filtered through pre-flushed 0.45 μm cellulose acetate filter.

Fluorescence and absorbance were measured simultaneously in a 1 cm quartz cuvette at 20 °C using an Aqualog spectrofluorometer (Horiba Scientific). Excitation and emission matrices (EEMs) were collected with 2 s integration time with excitation wavelengths spanned from 240 to 650 nm in 3 nm increments and emission wavelengths spanned from 249 to 700 nm in 2.33 nm increments. Blank EEMs were acquired daily using both a sealed water blank and a Milli-Q sample.

Using parallel factor analysis (PARAFAC), fluorescence EEMs were decomposed to underlying fluorescence spectra ('components') and the relative intensity of each component ('score').[29] PARAFAC modelling was conducted using the *N-way* and drEEM toolboxes for MATLAB.[30,31] Prior to modelling, the EEM dataset (n = 18) was processed to remove the Raman and Rayleigh scatter bands and correct for inner filter effects and fluorescence intensities were converted to Raman units (RU). A four-component PARAFAC model explained 99.9% of the total variance in the EEM dataset (ESI† Fig. A4). Three identified components have fluorescence spectra characteristic of humic-like organic matter: C_1 ($\lambda_{ex/em}$: 320/410 nm), C_2 ($\lambda_{ex/em}$: 360/460 nm), C_4 ($\lambda_{ex/em}$: 420/510 nm). Another is characteristic of protein-like fluorescence: C_3 ($\lambda_{ex/em}$: 290/390 nm).

Fluorescence index (FI) was also calculated for each sample using the ratio of fluorescence emission intensity (470 nm/520 nm) at 370 nm excitation.[32] Fluorescence index (FI) is frequently used to infer the DOM source with low ratios (~1.2) indicating terrestrially-dominated NOM sources and high ratios (~1.8) indicating predominantly microbial sources.[33] All samples had similar FI values with the averaged value of 1.57 ± 0.01 suggesting that microbial sources were slightly more dominant than terrestrial sources for the DOM in the studied sampling sites.

All samples were tested for total organic carbon (TOC) and UV absorbance (UVA) using a TOC analyser (TOC-L,

Shimadzu) and spectrophotometer (DR 5000, Hach Lange), respectively. TOC samples taken from the raw water, basin A and B were filtered through a cell strainer (40 μm) before the analyses. The UVA was measured at λ = 254 nm using a 5 cm cuvette, which is the same sample protocol as used in the WTP. Specific ultraviolet absorbance (SUVA) was calculated as the ratio of UVA and TOC (UVA/TOC) and is referred to as $SUVA_{TOC}$. The percentage dissolved organic matter (DOC) in TOC from Lake Vomb was about 93% ± 5%.

2.3.3 Statistical analysis. Non-metric multidimensional scaling (NMDS) is an ordination technique based on distance or dissimilarity.[34] NMDS was used to visualize the differences in microbial communities based on infiltration basin performance, where the data was taken from gated populations of flow cytometric dot plots, as seen in ref. 12. The statistical calculations were conducted in R[35] using flowCORE and modified flowCHIC packages through a script developed by Niklas Gador at Kristianstad University, Sweden. Because all flow cytometric samples had vastly different cell counts (*i.e.* raw water samples as opposed to infiltrated water samples), the script randomly selected events equivalent to the sample with the lowest event count. For testing differences in treatment performance, Pearson correlation coefficient calculations and Student's *t*-tests were conducted.

3 Results

3.1 NOM removal efficiency

In this section, the results from the chemical parameters (TOC, UVA, $SUVA_{TOC}$ and fluorescence spectroscopy) describe the water quality changes during infiltration. Fig. 2 shows the results from the TOC (Fig. 2a), UVA (Fig. 2b) and $SUVA_{TOC}$ (Fig. 2c) measurements depending on the raw water temperature.

The $SUVA_{TOC}$ (UVA : TOC ratio) is relatively constant for all samples up to about 20 °C, where an increase is observed (Fig. 2c). The opposite is seen in Fig. 2a, where TOC decreases when raw water temperatures are above 20 °C. This indicates a change in NOM composition depending on raw water temperature. The seasonal NOM changes in lakes likely caused by precipitation and microbial activity[36,37] could be an explanation for this trend. Over the whole study period, the raw water temperature was positively correlated to UVA (0.80 and $\rho < 0.05$) and $SUVA_{TOC}$ (0.60 and $\rho < 0.05$), and with no correlations to TOC. The temporal changes in the TOC of the source water were reflected by the TOC of the samples collected at 50 and 100 cm depth. This response illustrates the rapid infiltration rates and the sensitivity of the initially infiltrated water to changes in the raw water quality. The results from Fig. 2a and b also show a clear separation between samples taken from the raw water, basin A and B and the infiltrated water samples taken from the soil water samplers. There was a highly significant difference in TOC between the raw water and the infiltrated water, $\rho < 10^{-10}$, and on average 37.1% of the TOC content was removed within one meters biofiltration. The UVA difference between raw water and the average infiltrated water was also significant, $\rho < 10^{-10}$, and the reduction was on average 33.5%. The *t*-test showed that the TOC was likely removed to a larger extent than UVA ($\rho < 0.1$). There was a significant difference in UVA between the average of all infiltrated water samples from basin A compared to B (ρ_{UVA} = 0.011). The results also showed that the TOC was likely lower in the infiltrated water samples under basin A ($\rho < 0.1$). Lastly, there was no significant difference for TOC and UVA measurements between samplers, individual or average, in vertical line with each other, *e.g.* A3-50 and A3-100 or A-50 and A-100. The complete list of mean values, variance and *p*-values (one and two tailed tests) can be seen in ESI† Table A1.

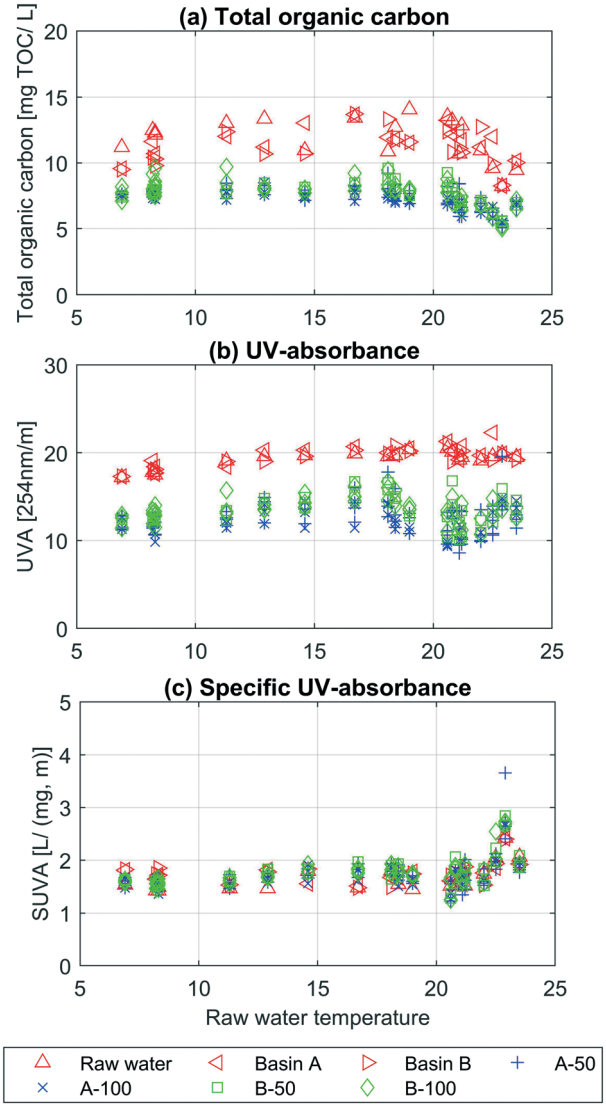

Fig. 2 Temperature effect on organic matter composition. The figure shows (a) TOC, (b) UVA and (c) the $SUVA_{TOC}$ for the raw water, basins and infiltrated water samples depending on the raw water temperature. The results are from the whole study period, July 4th to November 21st, 2018.

For three weeks from the 7th to 21st of November samples for fluorescence spectroscopy measurement were taken from the raw water and sampling points B3-50, B3-100, B4-50 and B4-100. The results from these measurements can be seen in ESI† Fig. A4. Fluorescent fraction of dissolved organic matter decreased significantly in the first 50 cm of the infiltration basin, being consistent with the results obtained from TOC and UVA. The fluorescence intensity of four PARAFAC

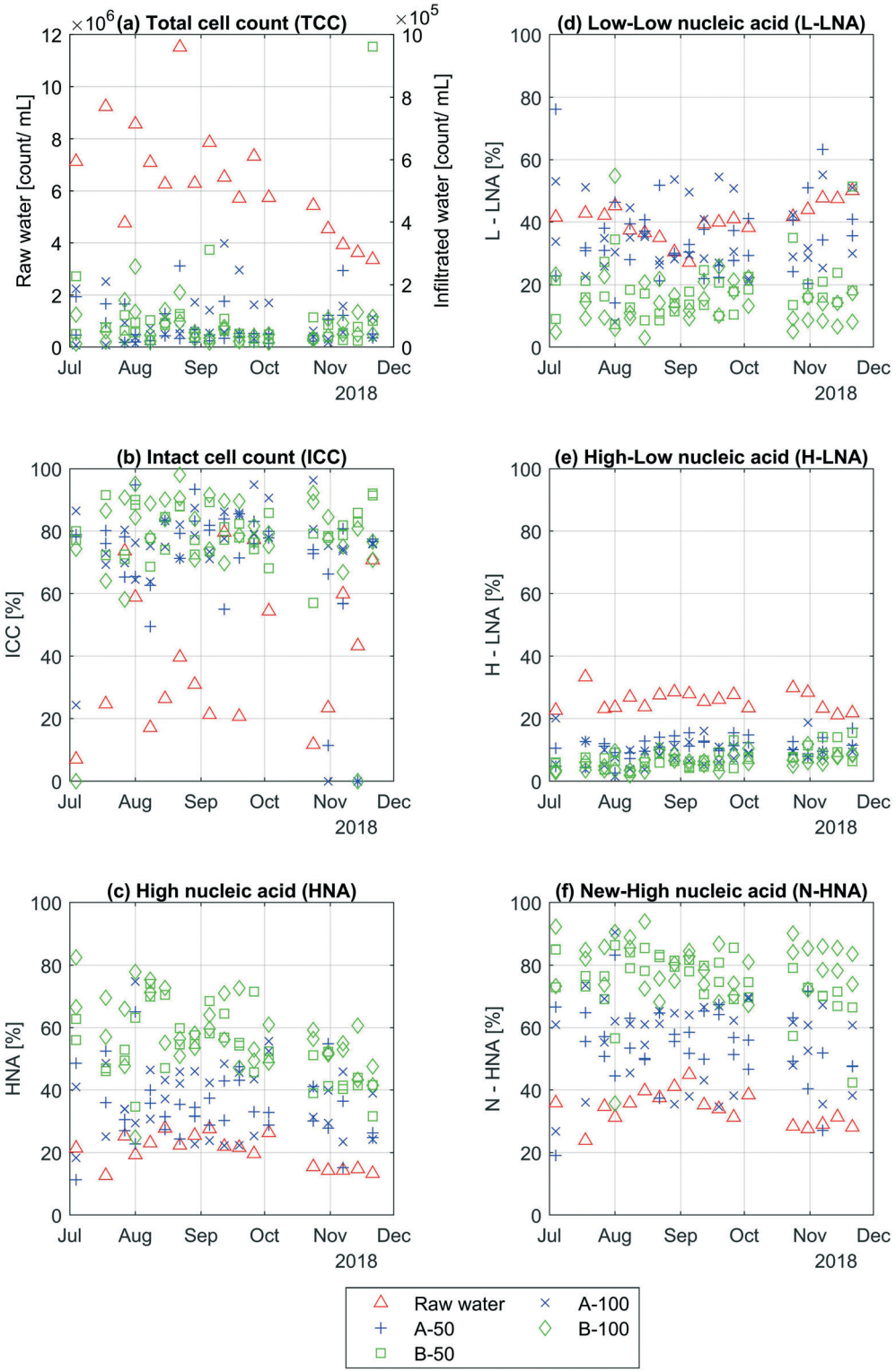

Fig. 3 Changes in bacterial communities. The figure shows (a) TCC, (b) % ICC, (c) % HNA, (d) % L-LNA, (e) % H-LNA and (f) % N-HNA from raw water and all individual soil water samplers.

components were compared between the raw water, 50 cm and 100 cm depths at both sampling locations (B3 and B4). Greater reduction was observed in protein-like component (C_3) compared to the three humic-like components with C_3 reducing between 33–35% in the first 50 cm while humic-like components (C_1, C_2 and C_4) reducing less than 21% (ESI† Table A1). The average TOC removal over the same three-week period was around 40% after the first 50 cm of the infiltration and remained unchanged in the second half of infiltration. Similar results were observed using the UVA-measurements, where UVA decrease with about 30% after the first 50 cm. This means that $SUVA_{TOC}$ increased after infiltration, which was also shown for the whole study period and implies preferential removal of non-aromatic compounds.

3.2 Bacteria community dynamics

This section shows the results from the flow cytometric measurements taken from the raw water, samplers A3-50, A3-100, A4-50, A4-100, B3-50, B3-100, B4-50 and B4-100. Fig. 3 shows the variations in TCC, % ICC, % HNA, % L-LNA, % H-LNA and % N-HNA over the whole period.

Fig. 3a shows that about 99% of cells were removed due to infiltration of raw water into the soil. The cell count in the raw water varies a lot each week, around 3×10^6 to 1×10^7 cells per mL over the whole period, especially during the mid to late summer months (July to September). Later in the year, the cell count in the raw water varied less and slowly decreases towards the end of the year. The cell count in the infiltrated water varied less, around 6×10^3 to 3×10^5 cells per mL, with one exception on the 21st of November. This sampling point, B3-50, showed a high cell count around 10^6 cells per mL. As seen in ESI† Table A2, the TCC in the raw water is significantly higher than the average TCC taken from the infiltrated water ($\rho < 10^{-9}$). There were no significant differences in TCC between all infiltrated water samples from A and B-side, and no significant change was observed in infiltrated water samples between 50 and 100 cm.

Similar to the TCC results, the percent ICC varied more in the raw water than the infiltrated water with a couple exceptions (Fig. 3b), one on the 4th of July (A4-100 at 24%) and one at the 31st of October (A3-50 at 11%). Overall, the ICC in the raw water varied between about 7 and 80% and was significantly lower ($\rho < 10^{-5}$) than the average percent infiltrated water ICC (ESI† Table A2), where the individual infiltrated water samples varied between 11 to 98%. On average, the % ICC was significantly higher in the infiltrated water samples under basin B (80%) compared with basin A (74%). The results also show that the % ICC stayed the same after 100 cm of infiltration.

Contrary to the TCC and % ICC, the % HNA varies more in the infiltrated water than in the raw water (Fig. 3c). Over the whole period, the % HNA in the raw water varies between 13 and 29% while the infiltrated water samples vary between 11 and 82%. As seen in ESI† Table A2, this increase in percent HNA in the raw water compared to the average HNA (%) in the infiltrated water was significant ($\rho < 10^{-16}$). All infiltrated water samples from under basin A contains significantly less % HNA than samples taken from under basin B (see ESI† Table A2), and significant changes with infiltration depth mostly occurred under basin B.

For % L-LNA, % H-LNA and % N-HNA, the infiltrated water under basin B had in general changed more during infiltration compared to the infiltrated water under basin A (-Fig. 3d–f). The % L-LNA had significantly decreased when comparing the raw water with all samplers from each side separately. There were however no changes between some of the individual infiltrated water samples from A-side and raw water, indicting less consistent performance of basin A. There was also a likely change between B-50 and B-100 (p = 0.11) and no change between A-50 and A-100. On average, the % L-LNA in the raw water, all infiltrated water samples under basin A and B were 40, 35 and 16%, where the % L-LNA was significantly lower in the infiltrated water under basin B compared to A (ESI† Table A2). Basin A and B performed similarly in reducing the % H-LNA, where the largest changed occurred during the first 50 cm followed by minor changes between 50 and 100 cm (ESI† Table A2). On average, infiltrated water samples under basin B had significantly lower % H-LNA compared to basin A. Similar to % HNA, the % N-HNA increase after infiltration from 34% in the raw water to 55% for A-side and to 77% for B-side. The % N-HNA also increased between the infiltrated water samples at 50 and 100 cm under basin B (p = 0.06) The same was not observed for samplers under basin A.

The similarities between the raw water and infiltrated water under basin A can be seen in the NMDS-plot in Fig. 4. Infiltrated water samples from both sides and raw water, form three overlapping groups. The NMDS-plot summerizes the previous results, without taking the fingerprint profiles (*i.e.* LNA, HNA *etc.*) into consideration, showing that samples from A-side are closer to the raw water than samples from the B-side. Similar to the bacterial fingerprint results in ESI† Fig. A3, the same exceptions are found closer to the raw water cluster (B3-50 and B4-100).

The study started in July and ended in November allowing for changes from summer to winter to be observed. During this time, the raw water temperature ranged from around 20 °C in the beginning to about 6 °C in the end. The results show that there were no correlations between raw water temperature and any bacterial community parameters (*e.g.* TCC, % ICC and % HNA) for all infiltrated water samples. However, there was a significant ($\rho < 0.05$) positive correlation between raw water TCC, HNA, L-LNA, H-LNA, N-HNA and raw water temperature (R^2_{TCC} = 0.50, R^2_{HNA} = 0.55, $R^2_{L\text{-}LNA}$ = 0.37, $R^2_{H\text{-}LNA}$ = 0.38 and $R^2_{N\text{-}HNA}$ = 0.47). The % HNA and % H-LNA significantly ($\rho < 0.05$) increased ($R^2_{\%HNA}$ = 0.33 and $R^2_{\%H\text{-}LNA}$ = 0.25) with raw water temperature and% L-LNA decreased with temperature ($R^2_{\%L\text{-}LNA}$ = 0.25, $\rho < 0.05$). The % N-HNA also likely increased

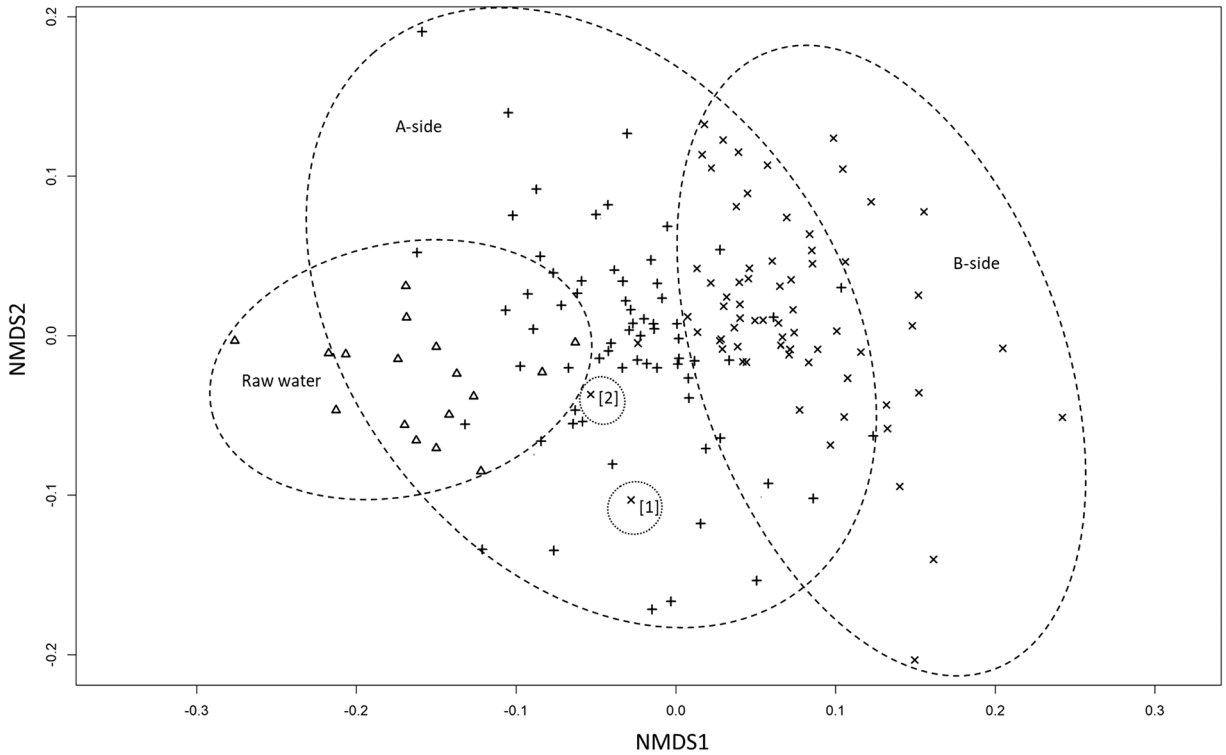

Fig. 4 Non-metric multidimensional scaling (NMDS) plot. Samples from the raw water (Δ), A (+) and B-side (x) are grouped shown by the three circles. The two exceptions with high TCCs from B-side are [1] B3-50 and [2] B4-100.

($R^2_{\%N\text{-}HNA}$ = 0.12, $\rho < 0.1$) with temperature. This shows that the bacteria with more DNA are increasing more than the bacteria with less DNA when raw water temperatures increase. An overview of all the results can be seen in ESI† Fig. A5.

4 Discussion

4.1 Differences in basin treatment performance

The performance of the two halves of the basin were very similar based on the TOC and UVA measurements. There was no significant difference after 50 cm of infiltration between the two halves. However, the UVA was significantly lower under basin A ($\rho < 0.05$) after 100 cm of infiltration. This suggests that NOM removal rates mostly depend on retention times rather than basin management. The different retention times in the recharge field comes from the natural variability of the geology in Vomb infiltration fields[38] and possibly from different infiltration rates in the unsaturated zone.[39]

The TCC in the infiltrated water samples showed that there were no significant differences in basin performance. However, the compositional changes in the microbial communities in the infiltrated water showed a substantial difference between the two basin halves. After 100 cm of infiltration, there were still no significant differences between the two basin halves overall. The similarities between samples under basin A and the raw water can clearly be seen in the NMDS-plot, where the groups are closely situated. The difference in basin performance was also shown in Fig. 3c–f, where infiltrated water samples under basin B moved further away from the raw water after infiltration. Even though the majority of bacterial community change occurred after 50 cm of infiltration on both sides, more significant change occurred between 50 and 100 cm under basin B compared to basin A (ESI† Table A2). The % ICC in the infiltrated water was also higher under basin B indicating differences in basin performance. This is a strong indication that basin management impacts the microbial community more than retention times in first meter of infiltration.

In summary, drying and freezing the basin resulted in significant differences in the bacterial community in the infiltrated water, and with on significant differences in the basins capacity to remove organic matter after the first meter of infiltration. Depending on the conditions, an argument could be made for both drying and not drying the infiltration basins. For Vomb Water Works, restarting the recharge to the basins directly after cleaning makes sense for a couple of reasons. Directly restarting basins would free up more surface area and at the same time limit high infiltration rates on small surface areas in the beginning, before a well-developed biofilm is established. Experiences from other WTPs in Sweden have shown that letting basins dry is not an option due to limited infiltration space.[9] On the other hand, drying the basin could be a viable option when the permeability of the infiltration field is low[40] or when using infiltration to create a hydraulic barrier.[41] However, drying the basins might negatively affect the microbial barrier and the increased permeability is likely only temporary.[42]

4.2 General water quality changes during infiltration

The high variation of ICC and TCC in the raw water samples (Fig. 3a and b) show the rapid changes in Lake Vomb, which might be influenced by the anthropogenic effects on the lake (*i.e.* nutrients from agriculture and wastewater from single households). After 50 cm of infiltration, TCC was removed by about 99%, through adsorption to the biofilm and the physical filtering effect of the soil pores (including the soil water samplers). This was in line with the observed NOM-reduction, where the most significant reduction occurred during the first 50 cm of infiltration. The large decrease of organic matter in the first 50 cm is predominately the removal of biodegradable fraction of NOM. This was observed in the fluorescence intensity of the four PARAFAC-components, where protein-like components were reduced to a larger extent than the humic-like components. The favourable reduction of protein-like components are likely due to adsorption and degradation, but could also be influenced by physical filtration.[43] The heterogenetic reduction of NOM is also supported by the observed likely increase in $SUVA_{TOC}$ from raw water to the infiltrated water samples, which is an indication of a higher reduction of biodegradable organic matter content.[44] In this case, TOC was reduced by about 37.1% and UVA by about 33.5% (p = 0.075). As discussed in McCarthy *et al.* (1996),[45] it is useful to look at NOM transport in terms of chemical heterogeneity rather than bulk transport. One interpretation drawn from this could be that raw water sources with higher SUVA values might benefit more from longer retention times (distance and time from recharge to extraction), and less from thick unsaturated zones. The opposite could be true for raw water sources with low SUVA values.

The average % ICC increased after infiltration and with no significant change between 50 and 100 cm. The increase in % ICC during infiltration was expected and has also been observed by Chan *et al.*, (2018)[12] and Lautenschlager *et al.*, (2014)[13] when measuring SSF influent and effluent. In these studies (when treating a pre-treated raw water with SSF) and what has been observed in the finished drinking water at Vomb WW,[46] the % HNA decreases after the SSFs and after artificial recharge. The feed water to a SSF differs from surface water used for managed aquifer recharge (MAR), where surface water is rich in biodegradable NOM and could support microbial growth, observed as an increase in HNA-bacteria. The observed % HNA increase may also be due to a majority removal of slow-growing LNA-bacteria from the raw water, and that the following weeks before groundwater abstraction, when biodegradable NOM is depleted, an exchange between the biofilm and groundwater occurs.

According to Chan *et al.* (2016)[46] the TCC in the raw water and the collected well water at Vomb WW were about $5.9 \times 10^6 \pm 4.7 \times 10^4$ and $4.6 \times 10^5 \pm 4.0 \times 10^3$, respectively. These results match what this study observed in the raw water however, the average TCC in the infiltrated water samples was 7.4×10^4 cells per mL (ESI† Table A2). This indicates that the interactions between the biofilm and the infiltrated water during the remaining time before extraction involves a shift of the microbial community towards LNA bacteria and an increase in TCC. The TCC increase between the infiltrated water and the well water could be growth of LNA bacteria and biofilm detachment.

4.3 NOM and microbial community interactions

For the infiltrated water samples, there were no correlations between raw water temperature and the presented variables. However, the microbial community in the raw water was strongly affected by raw water temperature. As the raw water temperature decreased so did the TCC and all subgroups (L-LNA, H-LNA, N-HNA and HNA), which would reflect the increase of biomass when temperature rises. The bacterial community in the raw water also changed over time, where the % L-LNA decreased and % H-LNA, % N-HNA and % HNA increased with increasing raw water temperature. At the same time, $SUVA_{TOC}$ (UVA : TOC ratio) increased in the higher temperature range (around 20 to 24 °C), which coincides with the summer months (July and August). This is likely influenced by the seasonal algae blooms that occur in Lake Vomb during July to September.[47] Higher cell counts in raw waters have also been observed during summer, in Finland.[4] We would argue that these results show the interaction between the microbial community and the change in organic matter composition in the raw water, where the larger species start to outcompete the smaller species during summer and that bioavailable organic carbon decreases in the raw water by accumulation in cells. Li *et al.* (2012)[48] suggested that DOC might have a strong influence on microbial community composition and diversity in managed aquifer recharge systems, which could suggest that the changes in raw water temperature and seasonal algae blooms, together with NOM dynamics could affect the bacterial communities in the groundwater. These results indicate that changes WTPs might impose to either reduce organic matter before infiltration (*e.g.* chemical flocculation) or changing of raw water sources, will affect the microbial communities and therefore also the performance of the infiltration process.

4.4 Infiltration basin monitoring

Based on the results, it would seem sensible to conduct sampling and chemical analysis on infiltrated water samples up to about 50 cm below the surface. This could of course vary in other cases, especially if infiltration rates are higher. Nonetheless, we would expect to detect noticeable NOM changes mostly in the topsoil layers. This was not true for changes in bacterial communities, where changes were detectable after 100 cm of infiltration. This could be an important aspect to consider when planning sampling strategies for artificial recharge when monitoring changes in NOM and bacterial communities.

The possible breakthrough on the 21th November in sampling point B3-50 was observed in the TCC, fingerprints and NMDS-plot (Fig. 3a, ESI† A3 and 4), which might be

useful in different situations. For online TCC measurements, breakthroughs would be easily detected by operators as was shown in Besmer and Hammes (2016).[15] At the same time, visualizing the bacterial community fingerprints might be a useful tool for operators to detect the breakthroughs that does not give high TCC values. In ESI† Fig. A2, there were two other samples that clearly deviated in sampling location B. These two samples were from B4-50 and B4-100, B4-100 showed high TCC values. B4-50 showed fingerprints resembling that of samples taken from A-side, but without high TCC values. This means that WTPs could benefit from monitoring the fingerprints and not only the TCC for possible irregularities. These exceptions also illustrate the uncertainty in water quality improvements in the early stages of treatment.

5 Conclusion

The results from this study highlights the importance of a well-developed top layer biofilm and unsaturated zone, where a majority of the removal of NOM and microorganisms occurred after 50 cm of infiltration. The main conclusions can be summarized as follows:

- Drying and freezing the basin negatively affected the performance of the basin when it comes to influencing the bacterial communities in the infiltrated water.
- The TCC was removed by about 99% after only 50 cm of infiltration.
- After the first 50 cm, TOC and UVA were removed by about 37.1 and 35.5%, respectively, resulting in a $SUVA_{TOC}$ (UVA : TOC ratio) increase.
- Protein-like components were reduced to a larger extent (33–35%) than the humic-like components (21%).

Conflicts of interest

There are no conflicts to declare.

Acknowledgements

The authors acknowledge Niklas Gador at Kristianstad University for the help visualizing the microbial community data, and Britt-Marie Pott, Tobias Persson and Sandy Chan at Sydvatten for their support and fruitful discussions throughout the project. The authors would also like to acknowledge Marie Baehr at EPFF AB for the flow cytometry support, and the Sydvatten staff at Ringsjö and Vomb Water Works for their technical support.

References

1 SWWA, Swedish Water Wastewater Assoc. SWWA, http://www.svensktvatten.se/Vattentjanster/Dricksvatten/Ravatten/, (accessed 12 July 2017).
2 C. Stefan and N. Ansems, Web-based global inventory of managed aquifer recharge applications, *Sustain. Water Resour. Manag.*, 2018, **4**, 153–162.
3 C. Sprenger, N. Hartog, M. Hernández, E. Vilanova, G. Grützmacher, F. Scheibler and S. Hannappel, Inventory of managed aquifer recharge sites in Europe: historical development, current situation and perspectives, *Hydrogeol. J.*, 2017, **25**, 1909–1922.
4 R. E. Kolehmainen, J. H. Langwaldt and J. A. Puhakka, Natural organic matter (NOM) removal and structural changes in the bacterial community during artificial groundwater recharge with humic lake water, *Water Res.*, 2007, **41**, 2715–2725.
5 WHO, *Assessing microbial safety of drinking water: Improving approaches and methods*, WHO, 2016.
6 A.-J. Lindroos, V. Kitunen, J. Derome and H.-S. Helmisaari, Changes in dissolved organic carbon during artificial recharge of groundwater in a forested esker in Southern Finland, *Water Res.*, 2002, **36**, 4951–4958.
7 D. B. Kleja, P.-O. Johansson, J. Skarbinski and J. P. Gustafsson, Reduction of natural organic matter and microorganisms in artificial groundwater recharge – Part 2: Experiments in column and pilot scales with filter sand and iron oxide coated olivine sand, Swedish Water Wastewater Assoc. SWWA, 2009.
8 B. Sundlöf and L. Kronqvist, Artificial Groundwater Recharge - State of the Art - Evaluation of twenty Swedish Plants, Swedish Water Wastewater Assoc. SWWA, 1992.
9 K. Hägg, K. M. Persson, T. Persson and Q. Zhao, Artificial recharge plants for drinking water supply – Groundwork for a manual for operation, Swedish Water Wastewater Assoc. SWWA, 2015.
10 P. Jokela, T. Eskola, T. Heinonen, U. Tanttu, J. Tyrväinen and A. Artimo, Raw Water Quality and Pretreatment in Managed Aquifer Recharge for Drinking Water Production in Finland, *Water*, 2017, **9**(2), 138.
11 U. Tanttu and P. Jokela, Sustainable drinking water quality improvement by managed aquifer recharge in Tuusula region, Finland, *Sustain. Water Resour. Manag.*, 2018, **4**, 225–235.
12 S. Chan, K. Pullerits, J. Riechelmann, K. M. Persson, P. Rådström and C. J. Paul, Monitoring biofilm function in new and matured full-scale slow sand filters using flow cytometric histogram image comparison (CHIC), *Water Res.*, 2018, **138**, 27–36.
13 K. Lautenschlager, C. Hwang, F. Ling, W.-T. Liu, N. Boon, O. Köster, T. Egli and F. Hammes, Abundance and composition of indigenous bacterial communities in a multi-step biofiltration-based drinking water treatment plant, *Water Res.*, 2014, **62**, 40–52.
14 S. Chan, K. Pullerits, A. Keucken, K. M. Persson, C. J. Paul and P. Rådström, Bacterial release from pipe biofilm in a full-scale drinking water distribution system, *npj Biofilms Microbiomes*, 2019, **5**, 9.
15 M. D. Besmer and F. Hammes, Short-term microbial dynamics in a drinking water plant treating groundwater with occasional high microbial loads, *Water Res.*, 2016, **107**, 11–18.

16 R. G. Niswonger, E. D. Morway, E. Triana and J. L. Huntington, Managed aquifer recharge through off-season irrigation in agricultural regions, *Water Resour. Res.*, 2017, **53**, 6970–6992.
17 D. Page, E. Bekele, J. Vanderzalm and J. Sidhu, Managed aquifer recharge (MAR) in sustainable urban water management, *Water*, 2018, **10**(3), 239–255.
18 J. Li, *PhD thesis*, Department of Water Resources Engineering, Lund Institute of Technology, Lund University, 2020.
19 G. Hansson, Artificial groundwater recharge - A method used in Swedish drinking water supply, Swedish Water Wastewater Assoc. SWWA, 2000.
20 S. Grünheid, G. Amy and M. Jekel, Removal of bulk dissolved organic carbon (DOC) and trace organic compounds by bank filtration and artificial recharge, *Water Res.*, 2005, **39**, 3219–3228.
21 D. Li, M. Alidina, M. Ouf, J. O. Sharp, P. Saikaly and J. E. Drewes, Microbial community evolution during simulated managed aquifer recharge in response to different biodegradable dissolved organic carbon (BDOC) concentrations, *Water Res.*, 2013, **47**, 2421–2430.
22 B.-M. Pott, N. Cronberg, H. Annadotter, S. Johnsson and G. Cronberg, Effect of nitrate addition on algae bloom, Swedish Water Wastewater Assoc. SWWA, 2009.
23 Sydvatten AB, Sydvatten - collaborating for public welfare, https://sydvatten.se/wp-content/uploads/2016/02/Sydvatten-in-English.pdf.
24 A. S. Persson, O. Olsson, M. Rundlöf and H. G. Smith, Land use intensity and landscape complexity—Analysis of landscape characteristics in an agricultural region in Southern Sweden, *Agric., Ecosyst. Environ.*, 2010, **136**, 169–176.
25 Länsstyrelsen i Skåne Län, Vombsjön, https://www.lansstyrelsen.se/download/18.6ae610001636c9c68e55840/1527064814580/Vombsjön.pdf, (accessed 25 September 2018).
26 S. Buckingham, E. Tipping and J. Hamilton-Taylor, Dissolved organic carbon in soil solutions: a comparison of collection methods, *Soil Use Manage.*, 2008, **24**, 29.
27 S. Gillespie, P. Lipphaus, J. Green, S. Parsons, P. Weir, K. Juskowiak, B. Jefferson, P. Jarvis and A. Nocker, Assessing microbiological water quality in drinking water distribution systems with disinfectant residual using flow cytometry, *Water Res.*, 2014, **65**, 224–234.
28 E. I. Prest, F. Hammes, S. Kötzsch, M. C. M. van Loosdrecht and J. S. Vrouwenvelder, Monitoring microbiological changes in drinking water systems using a fast and reproducible flow cytometric method, *Water Res.*, 2013, **47**, 7131–7142.
29 R. Bro, PARAFAC. Tutorial and applications, *Chemom. Intell. Lab. Syst.*, 1997, **38**, 149–171.
30 C. A. Andersson and R. Bro, The N-way Toolbox for MATLAB, *Chemom. Intell. Lab. Syst.*, 2000, **52**, 1–4.
31 K. R. Murphy, C. A. Stedmon, D. Graeber and R. Bro, Fluorescence spectroscopy and multi-way techniques. PARAFAC, *Anal. Methods*, 2013, **5**, 6557–6566.
32 R. M. Cory and D. M. McKnight, Fluorescence Spectroscopy Reveals Ubiquitous Presence of Oxidized and Reduced Quinones in Dissolved Organic Matter, *Environ. Sci. Technol.*, 2005, **39**, 8142–8149.
33 D. M. McKnight, E. W. Boyer, P. K. Westerhoff, P. T. Doran, T. Kulbe and D. T. Andersen, Spectrofluorometric Characterization of Dissolved Organic Matter for Indication of Precursor Organic Material and Aromaticity, *Limnol. Oceanogr.*, 2001, **46**, 38–48.
34 J. Kruskal, Multidimensional scaling by optimizing goodness of fit to a nonmetric hypothesis, *Psychometrika*, 1964, **29**, 1–27.
35 R Development Core Team, R: A language and environment for statistical computing, 2009.
36 T. Jiang, X. Chen, D. Wang, J. Liang, W. Bai, C. Zhang, Q. Wang and S. Wei, Dynamics of dissolved organic matter (DOM) in a typical inland lake of the Three Gorges Reservoir area: Fluorescent properties and their implications for dissolved mercury species, *J. Environ. Manage.*, 2018, **206**, 418–429.
37 N. Karapinar, V. Uyak, S. Soylu and T. Topal, Seasonal variations of NOM composition and their reactivity in a low humic water, *Environ. Prog. Sustainable Energy*, 2014, **33**, 962–971.
38 U. Czarniecka, Investigations of infiltration basins at the Vomb Water Plant: a study of possible causes of reduced infiltration capacity, *MPhil thesis*, Diss. Geol. Lund Univ., 2005.
39 M. Persson, S. Haridy, J. Olsson and J. Wendt, Solute transport dynamics by high-resolution dye tracer experiments—image analysis and time moments, *Vadose Zone J.*, 2005, **4**, 856–865.
40 H. Bouwer, Artificial recharge of groundwater: hydrogeology and engineering, *Hydrogeol. J.*, 2002, **10**, 121–142.
41 A. Jódar-Abellán, J. A. Albaladejo-García and D. Prats, Artificial groundwater recharge. Review of the current knowledge of the technique, *Revista de la Sociedad Geológica de España*, 2017, **30**(1), 85–96.
42 W. M. Schuh, Seasonal variation of clogging of an artificial recharge basin in a northern climate, *J. Hydrol.*, 1990, **121**, 193–215.
43 A. Baker, S. Elliott and J. R. Lead, Effects of filtration and pH perturbation on freshwater organic matter fluorescence, *Chemosphere*, 2007, **67**, 2035–2043.
44 S. Goel, R. M. Hozalski and E. J. Bouwer, Biodegradation of NOM: effect of NOM source and ozone dose, *J. - Am. Water Works Assoc.*, 1995, **87**, 90.
45 J. F. McCarthy, B. Gu, L. Liang, J. Mas-Pla, T. M. Williams and T.-C. J. Yeh, Field Tracer Tests on the Mobility of Natural Organic Matter in a Sandy Aquifer, *Water Resour. Res.*, 1996, **32**, 1223–1238.
46 S. Chan, J. Riechelmann, P. Buakhom, K. Pullerits, K. M. Persson, P. Rådström and C. J. Paul, in IWA Microbial Ecology in Water Engineering & Biofilms joint specialist conferenc, 2016.

47 J. Li, L. Parkefelt, K. M. Persson and H. Pekar, Improving cyanobacteria and cyanotoxin monitoring in surface waters for drinking water supply, *J. Water Secur.*, 2017, **3**, 2345–363005.
48 D. Li, J. O. Sharp, P. E. Saikaly, S. Ali, M. Alidina, M. S. Alarawi, S. Keller, C. Hoppe-Jones and J. E. Drewes, Dissolved Organic Carbon Influences Microbial Community Composition and Diversity in Managed Aquifer Recharge Systems, *Appl. Environ. Microbiol.*, 2012, **78**, 6819–6828.